

1 **Contrasting responses of phytoplankton productivity between coastal and offshore**  
2 **surface waters in the Taiwan Strait and the South China Sea to short-term seawater**  
3 **acidification**

4

5 Guang Gao<sup>1</sup>, Tifeng Wang<sup>1</sup>, Jiazhen Sun<sup>1</sup>, Xin Zhao<sup>1</sup>, Lifang Wang<sup>1</sup>, Xianghui Guo<sup>1</sup>,  
6 Kunshan Gao<sup>1,2\*</sup>

7 <sup>1</sup>State Key Laboratory of Marine Environmental Science & College of Ocean and Earth  
8 Sciences, Xiamen University, Xiamen 361005, China

9 <sup>2</sup>Co-Innovation Center of Jiangsu Marine Bio-industry Technology, Jiangsu Ocean  
10 University, Lianyungang 222005, China

11

12 \*Corresponding author: ksgao@xmu.edu.cn

13

14 **Abstract**

15 Seawater acidification (SA) has been documented to either inhibit or enhance or result in  
16 no effect on marine primary productivity (PP). In order to examine effects of SA in  
17 changing environments, we investigated the influences of SA (a decrease of 0.4 pH<sub>total</sub>  
18 units with corresponding CO<sub>2</sub> concentrations ranged 22.0–39.7 μM) on PP through  
19 deck-incubation experiments at 101 stations in the Taiwan Strait and the South China Sea  
20 (SCS), including the continental shelf and slope, as well as deep-water basin. The daily  
21 primary productivities in surface seawater under incident solar radiation ranged from 17–  
22 306 μg C (μg Chl *a*)<sup>-1</sup> d<sup>-1</sup>, with the responses of PP to SA being region-dependent and the  
23 SA-induced changes varying from -88% (inhibition) to 57% (enhancement). The  
24 SA-treatment stimulated PP in surface waters of coastal, estuarine and shelf waters, but  
25 suppressed it in the South China Sea basin. Such SA-induced changes in PP were  
26 significantly related to in situ pH and solar radiation in surface seawater, but negatively  
27 related to salinity changes. Our results indicate that phytoplankton cells are more  
28 vulnerable to pH drop in oligotrophic waters. Contrasting responses of phytoplankton  
29 productivity in different areas suggest that SA impacts on marine primary productivity  
30 are region-dependent and regulated by local environments.

31 **Keywords:** CO<sub>2</sub>; Taiwan Strait; seawater acidification; photosynthesis; primary  
32 productivity; South China Sea

33 **1 Introduction**

34 The oceans have absorbed about one-third of anthropogenically released CO<sub>2</sub>, which  
35 increased dissolved CO<sub>2</sub> and decreased pH of seawater (Gattuso et al., 2015), leading to  
36 ocean acidification (OA). This process is ongoing and likely intensifying (IPCC, 2019).  
37 OA has been shown to result in profound influences on marine ecosystems (see the  
38 reviews and literature therein, Mostofa et al., 2016; Doney et al., 2020). Marine  
39 photosynthetic organisms, which contribute about half of the global primary production,  
40 are also being affected by OA (see the reviews and literatures therein, Riebesell et al.,  
41 2018; Gao et al., 2019a). In addition to the slow change of ocean acidification, some  
42 processes, such as freshwater inputs, upwelling, typhoon and eddies, can lead to  
43 instantaneous CO<sub>2</sub> rising and seawater acidification (Moreau et al., 2017; Yu et al., 2020).  
44 Since seawater acidification occurs in many locations of ocean, it is important to  
45 understand the responses of the key players of marine biological CO<sub>2</sub> pump, the  
46 phytoplankton, to seawater acidification.

47 Elevated CO<sub>2</sub> is well recognized to lessen the dependence of algae and  
48 cyanobacteria on energy-consuming CO<sub>2</sub> concentrating mechanisms (CCMs) which  
49 concentrate CO<sub>2</sub> around Rubisco, the key site for photosynthetic carbon fixation (Raven  
50 & Beardall, 2014 and references therein; Hennon et al., 2015). The energy freed up from  
51 the down-regulated CCMs under increased CO<sub>2</sub> concentrations can be applied to other  
52 metabolic processes, resulting in a modest increase in algal growth (Wu et al., 2010;  
53 Hopkinson et al., 2011; Xu et al., 2017). Accordingly, elevated CO<sub>2</sub> availability could

54 potentially enhance marine primary productivity (Schippers et al., 2004). For instance,  
55 across 18 stations in the central Atlantic Ocean primary productivity was stimulated by  
56 15–19% under elevated dissolved CO<sub>2</sub> concentrations up to 36 μM (Hein and  
57 Sand-Jensen 1997). On the other hand, neutral effects of seawater acidification (SA) on  
58 growth rates of phytoplankton communities were reported in five of six CO<sub>2</sub>  
59 manipulation experiments in the coastal Pacific (Tortell et al., 2000). Furthermore,  
60 simulated future SA reduced surface PP in pelagic surface waters of Northern SCS and  
61 East China Sea (Gao et al., 2012). It seems that the impacts of SA on PP could be  
62 region-dependent. The varying effects of SA may be related to the regulation of other  
63 factors such as light intensity (Gao et al., 2012), temperature (Holding et al., 2015),  
64 nutrients (Tremblay et al., 2006) and community structure (Dutkiewicz et al., 2015).

65 Taiwan Strait of the East China Sea, located between southeast Mainland China and  
66 the Taiwan Island, is an important channel in transporting water and biogenic elements  
67 between the East China Sea (ECS) and the South China Sea (SCS). Among the Chinese  
68 coastal areas, the Taiwan Strait is distinguished by its unique location. In addition to  
69 riverine inputs, it also receives nutrients from upwelling (Hong et al., 2011). Primary  
70 productivity is much higher in coastal waters than that in basin zones due to increased  
71 supply of nutrients through river runoff and upwelling (Chen, 2003; Cloern et al., 2014).  
72 The South China Sea (SCS), located from the equator to 23.8 °N, from 99.1 to 121.1 °E  
73 and encompassing an area of about  $3.5 \times 10^6$  km<sup>2</sup>, is one of the largest marginal seas in

74 the world. As a marginal sea of the Western Pacific Ocean, it has a deep semi-closed  
75 basin (with depths > 5000 m) and wide continental shelves, characterized by a tropical  
76 and subtropical climate (Jin et al., 2016). Approximately 80% of ocean organic carbon is  
77 buried in the Earth's continental shelves and therefore continental margins play an  
78 essential role in the ocean carbon cycle (Hedges & Keil, 1995). Investigating how ocean  
79 acidification affects primary productivity in the Taiwan Strait and the SCS could help us  
80 to understand the contribution of marginal seas to carbon sink under the future  
81 CO<sub>2</sub>-increased scenarios. Although small-scale studies on SA impacts have been  
82 conducted in the ESC and the SCS (Gao et al., 2012, 2017), our understanding of how SA  
83 affects PP in marginal seas is still fragmentary and superficial. In this study, we  
84 conducted three cruises in the Taiwan Strait and the SCS, covering an area of  $8.3 \times 10^5$   
85 km<sup>2</sup>, and aimed to provide in-depth insight into how SA and/or episodic pCO<sub>2</sub> rise affects  
86 PP in marginal seas with comparisons to other types of waters.

## 87 **2 Materials and Methods**

### 88 **2.1 Investigation areas**

89 To study the impacts of projected SA (dropping by ~0.4 pH) by the end of this  
90 century (RCP8.5) on marine primary productivity in different areas (Gattuso et al., 2015),  
91 we carried out deck-based experiments during the 3 cruises supported by National  
92 Natural Science Foundation of China (NSFC), which took place in the Taiwan Strait (Jul  
93 14<sup>th</sup>–25<sup>th</sup>, 2016), the South China Sea basin (Sep 6–24<sup>th</sup>, 2016), and the West South China

94 Sea (Sep 14<sup>th</sup> to Oct 24<sup>th</sup>, 2017), respectively. The experiments were conducted at 101  
95 stations with coverage of 12 °N–26 °N and 110 °E–120 °E (Fig. 1). Investigation areas  
96 include the continental shelf (0–200 m, 22 stations) and the slope (200–3400 m, 44  
97 stations), and the vast deep-water basin (> 3400 m, 35 stations). In the continental shelf,  
98 the areas with depth < 50 m are defined as coastal zones (9 stations).

## 99 **2.2 Measurements of temperature and carbonate chemistry parameters**

100 The temperature and salinity of surface seawater at each station were monitored with  
101 an onboard CTD (Seabird, USA).  $\text{pH}_{\text{NBS}}$  was measured with an Orion 2-Star pH meter  
102 (Thermo scientific, USA) that was calibrated with standard National Bureau of Standards  
103 (NBS) buffers ( $\text{pH}=4.01, 7.00, \text{ and } 10.01$  at  $25.0\text{ }^{\circ}\text{C}$ ; Thermo Fisher Scientific Inc., USA).  
104 After the calibration, the electrode of pH meter was kept in surface seawater for half an  
105 hour and then the formal measurements were conducted. The analytical precision was  
106  $\pm 0.001$ . Total alkalinity (TA) was determined using Gran titration on a 25-mL sample  
107 with a TA analyzer (AS-ALK1, Apollo SciTech, USA) that was regularly calibrated with  
108 certified reference materials supplied by A. G. Dickson at the Scripps Institution of  
109 Oceanography (Gao et al., 2018a). The analytical precision was  $\pm 2\ \mu\text{mol kg}^{-1}$ .  $\text{CO}_2$   
110 concentration in seawater and the  $\text{pH}_{\text{Total}}$  ( $\text{pH}_{\text{T}}$ ) values was calculated by using CO2SYS  
111 (Pierrot et al., 2006) with the input of  $\text{pH}_{\text{NBS}}$  and TA data.

## 112 **2.3 Solar radiation**

113 The incident solar radiation intensity during the cruises was recorded with an

114 Eldonet broadband filter radiometer (Eldonet XP, Real Time Computer, Germany). This  
115 device has three channels for PAR (400–700 nm), UV-A (315–400 nm) and UV-B (280–  
116 315 nm) irradiance, respectively, which records the means of solar radiations over each  
117 minute. The instrument was fixed at the top layer of the ship to avoid shading.

#### 118 **2.4 Determination of primary productivity**

119 Surface seawater (0–1m) was collected a 10 L acid-cleaned (1 M HCl) plastic bucket  
120 and pre-filtered (200 µm mesh size) to remove large grazers. To prepare high CO<sub>2</sub> (HC)  
121 seawater, CO<sub>2</sub>-saturated seawater was added into pre-filtered seawater until a decrease of  
122 ~0.4 units in pH (corresponding CO<sub>2</sub> concentrations being 22.0–39.7 µM) was  
123 approached (Gattuso et al., 2010). Seawater that was collected from the same location as  
124 PP and filtered by cellulose acetate membrane (0.22 µm) was used to make the  
125 CO<sub>2</sub>-saturated seawater, which was made by directly flushing with pure CO<sub>2</sub> until pH  
126 reached around 4.50. When saturated-CO<sub>2</sub> seawater was added to the HC treatment,  
127 equivalent filtered seawater (without flushing with CO<sub>2</sub>) was also added to the AC  
128 treatment as a control. The ratios of added saturated-CO<sub>2</sub> seawater to incubation seawater  
129 were about 1:1000. Seawater was incubated within half an hour after they were collected.  
130 Prepared AC and HC seawater was allocated into 50-mL quartz tubes in triplicate,  
131 inoculated with 5 µCi (0.185 MBq) NaH<sup>14</sup>CO<sub>3</sub> (ICN Radiochemicals, USA), and then  
132 incubated for 24 h (over a day-night cycle) under 100 % incident solar irradiances in a  
133 water bath for temperature control by running through surface seawater. Due to heating

134 by the deck, the temperatures in the water bath were 0–2 °C higher than in situ surface  
135 seawater temperatures. TA and pH of seawater before and after 24h incubation were  
136 measured to monitor the changes of carbonate systems. After the incubation, the cells  
137 were filtered onto GF/F filters (Whatman) and immediately frozen at –20 °C for later  
138 analysis. In the laboratory, the frozen filters were transferred to 20 mL scintillation vials,  
139 thawed and exposed to HCl fumes for 12 h, and dried (55 °C, 6 h) to expel non-fixed <sup>14</sup>C,  
140 as previously reported (Gao et al., 2017). Then 3 mL scintillation cocktail (Perkin  
141 Elmer®, OptiPhase HiSafe) was added to each vial. After 2 h of reaction, the  
142 incorporated radioactivity was counted by a liquid scintillation counting (LS 6500,  
143 Beckman Coulter, USA). The carbon fixation for 24 h incubation was taken as  
144 chlorophyll (Chl) *a*-normalized daily primary productivity (PP, µg C (µg Chl *a*)<sup>-1</sup>) (Gao et  
145 al., 2017). The changes (%) of PP induced by ocean acidification were expressed as  
146  $(PP_{HC}-PP_{AC})/PP_{AC}\times 100$ , where PP<sub>HC</sub> and PP<sub>AC</sub> are the daily primary productivity under  
147 HC and AC, respectively.

## 148 **2.5 Chl *a* measurement**

149 Pre-filtered (200 µm mesh size) surface seawater (500–2000 mL) at each station was  
150 filtered onto GF/F filter (25 mm, Whatman) and then stored at -80 °C. After returning to  
151 laboratory, phytoplankton cells on the GF/F filter were extracted overnight in absolute  
152 methanol at 4 °C in darkness. After centrifugation (5000 g for 10 min), the absorption  
153 values of the supernatants were analyzed by a UV–VIS spectrophotometer (DU800,



154 Beckman, Fullerton, California, USA). The concentration of chlorophyll *a* (Chl *a*) was  
155 calculated according to Porra (2002).

## 156 **2.6 Data analysis**

157 The data of environmental parameters were expressed in raw and the data of PP were  
158 the means of triplicate incubations. Two-way analysis of variance (ANOVA) was used to  
159 analyze the effects of SA and location on PP. Least significant difference (LSD) was used  
160 to for *post hoc* analysis. Linear fitting analysis was conducted with Pearson correlation  
161 analysis to assess the relationship between PP and environmental factors. A 95%  
162 confidence level was used in all analyses.

## 163 **3 Results**

164 During the cruises, surface temperature ranged from 25.0 to 29.9 °C in the Taiwan  
165 Strait and from 27.1 to 30.2 °C in the South China Sea (Fig. 2a). Surface salinity ranged  
166 from 30.0 to 34.0 in the Taiwan Strait and from 31.0 to 34.3 in the South China Sea (Fig.  
167 2b). The lower salinities were found in the estuaries of Minjiang and Jiulong Rivers as  
168 well as Mekong River-induced Rip current. High salinities were found in the SCS basin.  
169 Surface pH<sub>T</sub> changed between 7.99–8.20 in the Taiwan Strait with the higher values in  
170 the estuary of Minjiang River (Fig. 2c). Compared to the Taiwan Strait, the South China  
171 Sea had lower surface pH (7.91–8.08) with the lowest value near the island in the  
172 Philippines. TA ranged from 2100 to 2359 μmol kg<sup>-1</sup> SW in the Taiwan Strait and 2126 to  
173 2369 μmol kg<sup>-1</sup> SW in the South China Sea (Fig. 2d). The lowest value occurred in the

174 estuary of Minjiang River. CO<sub>2</sub> concentration in surface seawater changed from 6.4–13.3  
175 μM kg<sup>-1</sup> SW in the Taiwan Strait, and 9.3–14.3 μM kg<sup>-1</sup> SW in the SCS (Fig. 1e). It  
176 showed an opposite pattern to surface pH, with the lowest value in the estuary of  
177 Minjiang River in the Taiwan Strait and highest value in near the islands in the  
178 Philippines in the South China Sea. During the PP investigation period, the daytime mean  
179 PAR intensity ranged from 126.6 to 145.2 W m<sup>-2</sup> s<sup>-1</sup> in the Taiwan Strait and 37.3 to 150.0  
180 W m<sup>-2</sup> s<sup>-1</sup> in the SCS (Fig. 2f).

181 The concentration of Chl *a* ranged from 0.11 to 12.13 μg L<sup>-1</sup> in the Taiwan Strait (Fig.  
182 3). The highest concentration occurred in the estuary of the Minjiang River. The  
183 concentration of Chl *a* in the SCS ranged from 0.037 to 7.43 μg L<sup>-1</sup>. The highest  
184 concentration was found in the coastal areas of Guangdong province in China. For both  
185 the Taiwan Strait and the SCS, there were high Chl *a* concentrations (> 1.0 μg L<sup>-1</sup>) in  
186 coastal areas, particularly in the estuaries of the Minjing River, Jiulong River and Pearl  
187 River. On the contrary, Chl *a* concentrations in offshore areas were lower than 0.2 μg L<sup>-1</sup>.

188 Surface primary productivity changed from 99–302 μg C (μg Chl *a*)<sup>-1</sup> d<sup>-1</sup> in the  
189 Taiwan Strait, and from 17–306 μg C (μg Chl *a*)<sup>-1</sup> d<sup>-1</sup> in the South China Sea (Fig. 4).  
190 High surface primary productivity (> 200 μg C (μg Chl *a*)<sup>-1</sup> d<sup>-1</sup>) was found in the  
191 estuaries of the Minjing River, Jiulong River, and Pearl River and areas near the East of  
192 Vietnam. In basin zones, the surface primary productivity was usually lower than 100 μg  
193 C (μg Chl *a*)<sup>-1</sup> d<sup>-1</sup>.

194 A series of onboard CO<sub>2</sub>-enrich experiments in the investigated regions were  
195 conducted during three cruises. In the high CO<sub>2</sub> treatments, pH<sub>total</sub> had a decrease of  
196 0.34–0.43 units, while pCO<sub>2</sub> and CO<sub>2</sub> had an increase of 676–982 μatm and 17–25 μM  
197 kg<sup>-1</sup> SW, respectively (Table S1). Carbonate chemistry parameters after 24 h of  
198 incubation were stable ( $\Delta$ pH < 0.06,  $\Delta$ TA < 53 μmol kg<sup>-1</sup> SW), indicating the  
199 successful manipulation (Table S1). It was observed that instantaneous effects of elevated  
200 pCO<sub>2</sub> on primary productivity of surface phytoplankton community in all investigated  
201 regions ranged from -88% (inhibition) to 57% (promotion), revealing significant regional  
202 differences (ANOVA,  $F_{(100, 404)} = 4.103$ ,  $p < 0.001$ , Fig. 5). Among 101 stations, 70  
203 stations showed insignificant SA effects. SA increased PP at 6 stations and reduced PP at  
204 25 stations. Positive effects of SA on surface primary productivity were observed in the  
205 Taiwan Strait and the western SCS (Fig. 5, red-yellow shading areas), with the maximal  
206 enhancement of 57% in the station approaching the Mekong River plume (LSD,  $p <$   
207 0.001). Reductions in PP induced by the elevated CO<sub>2</sub> were mainly found in the central  
208 SCS basin within the latitudes of 10 °N to 14 °N and the longitudes of 114.5 °E to 118 °E  
209 (Fig. 5, blue-purple shading areas), with inhibition rates ranging from 24% to 88% (Fig. 5,  
210 LSD,  $p < 0.05$ ). These results showed a region-related effect of SA on photosynthetic  
211 carbon fixation of surface phytoplankton assemblages. Overall, the elevated pCO<sub>2</sub> had  
212 neutral or positive effects on primary productivity in the continental shelf and slope  
213 regions, while having adverse effects in the deep-water basin.

214 By analyzing the correlations between SA-induced PP changes and regional  
215 environmental parameters, we found that SA-induced changes in phytoplankton primary  
216 productivity was significantly positively related with *in situ* pH ( $p < 0.001$ ,  $r = 0.379$ ),  
217 and PAR density ( $p = 0.002$ ,  $r = 0.311$ ) (Fig. 6 and Table S1). On the other hand, the  
218 influence induced by SA was negatively related to salinity that ranged from 30.00 to  
219 34.28 ( $p < 0.001$ ,  $r = -0.418$ ).

#### 220 **4 Discussion**

221 In the present study, we found that the elevated pCO<sub>2</sub> and associated pH drop  
222 increased or did not affect PP in the continental shelf and slope waters but reduced it in  
223 basin waters. Our results suggested that the enhanced effects of the SA treatment on  
224 photosynthetic carbon fixation depend on regions of different physicochemical conditions,  
225 including pH, light intensity and salinity. In addition, coastal diatoms appear to benefit  
226 more from SA than pelagic ones (Li et al., 2016). Therefore, community structure  
227 differences might also be responsible for the differences of the short-term high  
228 CO<sub>2</sub>-induced acidification between coastal and basin waters.

229 SA is deemed to have two kinds of effects at least (Xu et al., 2017; Shi et al., 2019).  
230 The first one is the enrichment of CO<sub>2</sub>, which is usually beneficial for photosynthetic  
231 carbon fixation and growth of algae because insufficient ambient CO<sub>2</sub> limits algal  
232 photosynthesis (Hein & Sand-Jensen, 1997; Bach & Taucher, 2019). The other effect is  
233 the decreased pH which could be harmful because it disturbs the acid-base balance

234 between extracellular and intracellular environments. For instance, the decreased pH  
235 projected for future SA was shown to reduce the growth of the diazotroph *Trichodesmium*  
236 (Hong et al., 2017), decrease PSII activity by reducing the removal rate of PsbD (D2)  
237 (Gao et al., 2018b) and increase mitochondrial and photo-respirations in diatoms and  
238 phytoplankton assemblages (Yang and Gao 2012, Jin et al., 2015). In addition, SA could  
239 reduce the Rubisco transcription of diatoms, which also contributed to the decreased  
240 growth (Endo et al., 2015). Therefore, the net impact of SA depends on the balance  
241 between its positive and negative effects, leading to enhanced, inhibited or neutral  
242 influences, as reported in diatoms (Gao et al., 2012, Li et al., 2021) and phytoplankton  
243 assemblages in the Arctic and subarctic shelf seas (Hoppe et al., 2018), the North Sea  
244 (Eberlein et al., 2017) and the South China Sea (Wu and Gao 2010, Gao et al., 2012). The  
245 balance of positive and negative effects of SA can be regulated by other factors, including  
246 pH, light intensity, salinity, population structure, etc. (Gao et al., 2019a, b; Xie et al.,  
247 2022).

248 In the present study, SA increased or did not affect PP in coastal waters but reduced it  
249 in offshore waters, which is significantly related to pH, light intensity and salinity (Fig. 6).  
250 The effect of SA changed from negative to positive with the increase of local pH. The  
251 higher pH occurred in coastal zones which may be caused by higher biomass of  
252 phytoplankton (Fig. 3). Higher pH caused by intensive photosynthesis of phytoplankton  
253 is accompanied with decreased CO<sub>2</sub> levels. In this case, CO<sub>2</sub> is more limited for

254 photosynthesis of phytoplankton compared to lower pH. Therefore, SA could stimulate  
255 primary productivity via supplying more available CO<sub>2</sub> (Hurd et al., 2019). On the other  
256 hand, lower pH occurred in deep-water basin. Lower pH represents higher CO<sub>2</sub>  
257 availability. CO<sub>2</sub> is not limited or less limited in this case. Therefore, more CO<sub>2</sub> brought  
258 by SA may not benefit photosynthesis of phytoplankton. Instead, decreased pH  
259 accompanied by SA may inhibit photosynthesis or growth of phytoplankton, which is  
260 found in cyanobacteria (Hong et al., 2017). Furthermore, the negative effects of SA are  
261 particularly significant when nutrient is limited (Li et al., 2018). The nutrient levels in  
262 basin are usually lower than shelf (Yuan et al., 2011; Lu et al., 2020; Du et al., 2021),  
263 which may exacerbate the negative effects of OA in the basin zone.

264       The negative effects of SA disappeared with the increase of light intensity in this  
265 study. This results in inconsistent with Gao et al (2012)' study, in which SA increased  
266 photosynthetic carbon fixation of three diatoms (*Phaeodactylum tricornutum*,  
267 *Thalassiosira pseudonana* and *Skeletonema costatum*) under lower light intensities but  
268 increased it under higher light intensities. The divergent findings may be due to different  
269 population structure that varies in different areas. Coastal zones where nutrients are  
270 relatively sufficient usually have abundant diatoms while picophytoplanktons mainly  
271 *Prochlorococcus* and *Synechococcus*, dominate oligotrophic areas (Xiao et al., 2018,  
272 Zhong et al., 2020). In this study, most investigated areas are oligotrophic and thus the  
273 response of local phytoplankton to the combination of light intensity and SA may be

274 different from diatoms. It is worth noting that the samples were not mixed down in the  
275 water bath in the present study and the 100% incident solar irradiances may have high  
276 light stress on cells. Lower incident solar irradiances or some devices can be used to  
277 simulate seawater mixing in future studies. Negative correlation between SA-induced  
278 changes of PP and salinity was found in this study. The decrease of salinity (from 35 to  
279 30) has been shown to alleviate the negative effect of SA on photosynthetic carbon  
280 fixation of a coccolithorophorid *Emiliana huxleyi* (Xu et al., 2020) although the potential  
281 mechanisms remain unknown. On the other hand, the change of salinity (from 6 to 3) did  
282 not affect effective quantum yield of microplanktonic community in the Baltic Sea grown  
283 under different CO<sub>2</sub> levels (Wulff et al., 2018). In this study, we presume that the negative  
284 relationship between salinity and SA effects may be mainly related to local pH because  
285 lower salinity occurred in coastal waters where seawater pH was higher while the basin  
286 zone had higher salinities and lower pH.

287         The specific environmental conditions have profound effects on shaping diverse  
288 dominant phytoplankton groups (Boyd et al., 2010). Larger eukaryotic groups (especially  
289 diatoms) usually dominate the complex coastal regions, while picophytoplanktons  
290 (*Prochlorococcus* and *Synechococcus*), characterizing with more efficient nutrients  
291 uptake, dominate the relatively stable offshore waters (Dutkiewicz et al., 2015). In  
292 summer and early autumn, previous investigations demonstrated that diatoms dominated  
293 in the northern waters and the Taiwan Strait (coastal and shelf regions) with the high

294 abundance of phytoplankton, which are consistent with our Chl *a* data; *Prochlorococcus*  
295 and *Synechococcus* dominated in the SCS basin and the north of SCS (slope and basin  
296 regions) (Xiao et al., 2018, Zhong et al., 2020). In addition, it has been reported that  
297 larger cells benefit more from SA because a thicker diffusion layer around the cells limits  
298 the transport of CO<sub>2</sub> (Feng et al., 2010; Wu et al., 2014). In contrast, a thinner diffusion  
299 layer and higher surface to volume ratio in smaller phytoplankton cells can make them  
300 easier to transport CO<sub>2</sub> near the cell surface and within the cells, and therefore  
301 picophytoplankton species are less CO<sub>2</sub>-limited (Bao and Gao, 2021). Therefore, different  
302 community structures between coastal and basin areas could also be responsible for the  
303 enhanced and inhibitory effects of SA. It is worth noting that seasonality may also lead to  
304 the differential effects of SA on primary productivity since the Taiwan Strait cruise was  
305 conducted in July and the cruises of the South China Sea basin and the West South China  
306 Sea were conducted in September. The SST and solar PAR intensity of the Taiwan Strait  
307 in July was 2–3 °C and  $22 \pm 22 \text{ W m}^{-2} \text{ s}^{-1}$  higher than that in September (Zhang et al.,  
308 2008, 2009; Table S3). Although the effects of SA were not related to temperature as  
309 shown in this study (Table S2), the higher solar radiation in July may contribute to the  
310 positive effect of SA on primary productivity.

## 311 **5 Conclusions**

312 By investigating the impacts of the elevated pCO<sub>2</sub> on PP in the Taiwan Strait and the  
313 SCS, we demonstrated that such short SA-treatments induced changes in PP were mainly



314 related to pH, light intensity and salinity based on Pearson correlation coefficients,  
315 supporting the hypothesis that negative impacts of SA on PP increase from coastal to  
316 basin waters (Gao et al., 2019a). In view of ocean climate changes, strengthened  
317 stratification due to global warming would reduce the upward transports of nutrients and  
318 thus marine primary productivity. The negative effect of SA in basin zones would further  
319 reduce primary productivity. Meanwhile, PP in coastal waters would be increased by  
320 SA. .

321 *Data availability.* All data are included in the article or Supplement.

322 *Author contributions.* KG and TW developed the original idea and designed research.  
323 TW and JS carried out fieldwork. GG provided statistical analyses and prepared figures.  
324 GG, KG, and XZ wrote the manuscript. All contributed to revising the paper.

325 *Competing interests.* The contact author has declared that neither they nor their  
326 co-authors have any competing interests.

327 *Disclaimer.* Publisher's note: Copernicus Publications remains neutral with regard to  
328 jurisdictional claims in published maps and institutional affiliations.

329 *Acknowledgements.* This work was supported by the National Natural Science  
330 Foundation of China (41720104005, 41890803 and 42076154) and the Fundamental  
331 Research Funds for the Central Universities (20720200111). The authors are grateful to  
332 the students He Li, Xiaowen Jiang and Shanying Tong, and the laboratory technicians  
333 Xianglan Zeng and Wenyan Zhao. We appreciate the NFSC Shiptime Sharing Project

334 (project number: 41849901) for supporting the Taiwan Strait cruise (NORC2016-04). We  
335 appreciate the chief scientists Yihua Cai, Huabin Mao and Chen Shi and the R/V Yanping  
336 II, Shiyuan I and Shiyuan III for leading and conducting the cruises.

### 337 **References**

338 Bach, L. T., and Taucher, J.: CO<sub>2</sub> effects on diatoms: a synthesis of more than a decade of  
339 ocean acidification experiments with natural communities, *Ocean Sci.*, 15,  
340 1159-1175, 2019.

341 Bao, N., and Gao, K.: Interactive effects of elevated CO<sub>2</sub> concentration and light on the  
342 picophytoplankton *Synechococcus*, *Front. Mar. Sci.*, 8, 1-7, 2021.

343 Boyd, P. W., Strzepek, R., Fu, F. X., and Hutchins, D. A.: Environmental control of open-  
344 ocean phytoplankton groups: Now and in the future, *Limnol. Oceanogr.*, 55,  
345 1353-1376, 2010.

346 Chen, C. T. A.: Rare northward flow in the Taiwan Strait in winter: A note, *Cont. Shelf*  
347 *Res.*, 23, 387-391, 2003.

348 Cloern, J. E., Foster, S.Q. and Kleckner, A. E.: Phytoplankton primary production in the  
349 world's estuarine-coastal ecosystems, *Biogeosciences*, 11, 2477-2501, 2014.

350 Doney, S. C., Busch, D. S., Cooley, S. R., and Kroeker, K. J.: The impacts of ocean  
351 acidification on marine ecosystems and reliant human communities, *Annu. Rev. Env.*  
352 *Resour.*, 45, 83-112, 2020.

353 Du, C., He, R., Liu, Z., Huang, T., Wang, L., Yuan, Z., Xu, Y., Wang, Z. and Dai, M.:

354 Climatology of nutrient distributions in the South China Sea based on a large data  
355 set derived from a new algorithm. *Prog. Oceanogr.*, 195, 102586, 2021.

356 Dutkiewicz, S., Morris, J. J., Follows, M. J., Scott, J., Levitan, O., Dyhrman, S. T., and  
357 Berman-Frank, I.: Impact of ocean acidification on the structure of future  
358 phytoplankton communities, *Nat. Clim. Change*, 5, 1002-1006, 2015.

359 Eberlein, T., Wohlrab, S., Rost, B., John, U., Bach, L. T., Riebesell, U., and Van de Waal,  
360 D. B.: Effects of ocean acidification on primary production in a coastal North Sea  
361 phytoplankton community, *Plos One*, 12, 1-15, 2017.

362 Endo, H., Sugie, K., Yoshimura, T., and Suzuki, K.: Effects of CO<sub>2</sub> and iron availability  
363 on *rbcL* gene expression in Bering Sea diatoms, *Biogeosciences*, 12, 2247-2259,  
364 2015.

365 Feng, Y., Hare, C. E., Rose, J. M., Handy, S. M., DiTullio, G. R., Lee, P. A., Smith, W. O.,  
366 Peloquin, J., Tozzi, S., Sun, J., Zhang, Y., Dunbar, R. B., Long, M. C., Sohst, B.,  
367 Lohan, M., and Hutchins, D. A.: Interactive effects of iron, irradiance and CO<sub>2</sub> on  
368 Ross Sea phytoplankton, *Deep-Sea Res. PT. I*, 57, 368-383, 2010.

369 Flynn, K. J., Blackford, J. C., Baird, M. E., Raven, J. A., Clark, D. R., Beardall, J.,  
370 Brownlee, C., Fabian, H., and Wheeler, G. L.: Changes in pH at the exterior surface  
371 of plankton with ocean acidification, *Nat. Clim. Change*, 2, 510-513, 2012.

372 Gao, G., Xu, Z. G., Shi, Q., and Wu, H. Y.: Increased CO<sub>2</sub> exacerbates the stress of  
373 ultraviolet radiation on photosystem II function in the diatom *Thalassiosira*

374 *weissflogii*, Environ. Exp. Bot., 156, 96-105, 2018b.

375 Gao, G., Jin, P., Liu, N., Li, F. T., Tong, S. Y., Hutchins, D. A., and Gao, K. S.: The  
376 acclimation process of phytoplankton biomass, carbon fixation and respiration to the  
377 combined effects of elevated temperature and  $p\text{CO}_2$  in the northern South China Sea,  
378 Mar. Pollut. Bull., 118, 213-220, 2017.

379 Gao, G., Qu, L., Xu, T., Burgess, J.G., Li, X. and Xu, J.: Future  $\text{CO}_2$ -induced ocean  
380 acidification enhances resilience of a green tide alga to low-salinity stress. ICES J.  
381 Mar. Sci., 76, 2437-2445, 2019b.

382 Gao, G., Xia, J. R., Yu, J. L., Fan, J. L., and Zeng, X. P.: Regulation of inorganic carbon  
383 acquisition in a red tide alga (*Skeletonema costatum*): The importance of phosphorus  
384 availability, Biogeosciences, 15, 4871-4882, 2018a.

385 Gao, K. S., Beardall, J., Häder, D. P., Hall-Spencer, J. M., Gao, G., and Hutchins, D. A.:  
386 Effects of ocean acidification on marine photosynthetic organisms under the  
387 concurrent influences of warming, UV radiation, and deoxygenation, Front. Mar.  
388 Sci., 6, 1-18, 2019a.

389 Gao, K. S., Xu, J. T., Gao, G., Li, Y. H., Hutchins, D. A., Huang, B. Q., Wang, L., Zheng,  
390 Y., Jin, P., Cai, X. N., Hader, D. P., Li, W., Xu, K., Liu, N. N., and Riebesell, U.:  
391 Rising  $\text{CO}_2$  and increased light exposure synergistically reduce marine primary  
392 productivity, Nat. Clim. Change, 2, 519-523, 2012.

393 Gattuso, J. P., Gao, K. S., Lee, K., Rost, B., and Schulz, K. G.: Approaches and tools to

394 manipulate the carbonate chemistry, pp 41-52. Guide to best practices for ocean  
395 acidification research and data reporting, edited by: Riebesell, U., Fabry, V. J.,  
396 Hansson, L., and Gattuso J.-P., Luxembourg: Publications Office of the European  
397 Union, 2010.

398 Gattuso, J. P., Magnan, A., Bill é R., Cheung, W. W. L., Howes, E. L., Joos, F., Allemand,  
399 D., Bopp, L., Cooley, S. R., Eakin, C. M., Hoegh-Guldberg, O., Kelly, R. P., Portner,  
400 H. O., Rogers, A. D., Baxter, J. M., Laffoley, D., Osborn, D., Rankovic, A., Rochette,  
401 J., Sumaila, U. R., Treyer, S., and Turley, C.: Contrasting futures for ocean and  
402 society from different anthropogenic CO<sub>2</sub> emissions scenarios, *Science*, 349,  
403 aac4722, 2015.

404 Geider, R. J., La Roche, J., Greene, R. M., and Olaizola, M.: Response of the  
405 photosynthetic apparatus of *Phaeodactylum tricornutum* (Bacillariophyceae) to  
406 nitrate, phosphate, or iron starvation, *J. Phycol.*, 29, 755-766, 1993.

407 Häler, D. P., Williamson, C. E., W ängberg, S. A., Rautio, M., Rose, K. C., Gao, K. S.,  
408 Helbling, E. W., Sinha, R. P., and Worrest, R.: Effects of UV radiation on aquatic  
409 ecosystems and interactions with other environmental factors, *Photoch. Photobio.*  
410 *Sci.*, 14, 108-126, 2015.

411 Hedges, J. I., and Keil, R. G.: Sedimentary organic matter preservation: an assessment  
412 and speculative synthesis, *Mar. Chem.*, 49, 81-115, 1995.

413 Hein, M., and Sand-Jensen, K.: CO<sub>2</sub> increases oceanic primary production, *Nature*, 388,

414 526-527, 1997.

415 Hennon, G. M. M., Ashworth, J., Groussman, R. D., Berthiaume, C., Morales, R. L.,  
416 Baliga, N. S., Orellana, M. V., and Armbrust, E. V.: Diatom acclimation to elevated  
417 CO<sub>2</sub> via cAMP signalling and coordinated gene expression, *Nat. Clim. Change*, 5,  
418 761-765, 2015.

419 Hofmann, G. E., Smith, J. E., Johnson, K. S., Send, U., Levin, L. A., Micheli, F., Paytan,  
420 A., Price, N. N., Peterson, B., Takeshita, Y., Matson, P. G., Crook, E. D., Kroeker, K.  
421 J., Gambi, M. C., Rivest, E. B., Frieder, C. A., Yu, P. C., and Martz, T. R.:  
422 High-frequency dynamics of ocean pH: A multi-ecosystem comparison, *Plos One*, 6,  
423 1-11, 2011.

424 Holding, J. M., Duarte, C. M., Sanz-Martín, M., Mesa, E., Arrieta, J. M., Chierici, M.,  
425 Hendriks, I. E., Garcia-Corral, L. S., Regaudie-de-Gioux, A., Delgado, A., Reigstad,  
426 M., Wassmann, P., and Agusti, S.: Temperature dependence of CO<sub>2</sub>-enhanced  
427 primary production in the European Arctic Ocean, *Nat. Clim. Change*, 5, 1079-1082,  
428 2015.

429 Hong, H. S., Chai, F., Zhang, C. Y., Huang, B. Q., Jiang, Y. W., and Hu, J. Y.: An  
430 overview of physical and biogeochemical processes and ecosystem dynamics in the  
431 Taiwan Strait, *Cont. Shelf Res.*, 31, S3-S12, 2011.

432 Hong, H. Z., Shen, R., Zhang, F. T., Wen, Z. Z., Chang, S. W., Lin, W. F., Kranz, S. A.,  
433 Luo, Y. W., Kao, S. J., Morel, F. M. M. and Shi, D. L.: The complex effects of ocean

434 acidification on the prominent N<sub>2</sub>-fixing cyanobacterium *Trichodesmium*. *Science*,  
435 356, 527-530, 2017.

436 Hopkinson, B. M., Dupont, C. L., Allen, A. E., and Morel, F. M.: Efficiency of the  
437 CO<sub>2</sub>-concentrating mechanism of diatoms, *P. Natl. Acad. Sci. USA.*, 108, 3830-3837,  
438 2011.

439 Hoppe, C. J. M., Wolf, K. K. E., Schuback, N., Tortell, P. D., and Rost, B.: Compensation  
440 of ocean acidification effects in Arctic phytoplankton assemblages. *Nat. Clim.*  
441 *Change*, 8, 529-533, 2018.

442 Hurd, C.L., Beardall, J., Comeau, S., Cornwall, C.E., Havenhand, J.N., Munday, P.L.,  
443 Parker, L.M., Raven, J.A. and McGraw, C.M.: Ocean acidification as a multiple  
444 driver: how interactions between changing seawater carbonate parameters affect  
445 marine life. *Mari. Freshwater Res.*, 71, 263-274, 2019.

446 IPCC, 2019: IPCC Special Report on the Ocean and Cryosphere in a Changing Climate  
447 [H.-O. Pörtner, D.C. Roberts, V. Masson-Delmotte, P. Zhai, M. Tignor, E.  
448 Poloczanska, K. Mintenbeck, A. Alegría, M. Nicolai, A. Okem, J. Petzold, B. Rama,  
449 N.M. Weyer (eds.)]. In press.

450 Jin, P., Gao, G., Liu, X., Li, F. T., Tong, S. Y., Ding, J. C., Zhong, Z. H., Liu, N. N., and  
451 Gao, K. S.: Contrasting photophysiological characteristics of phytoplankton  
452 assemblages in the Northern South China Sea, *Plos One*, 11, 1-16, 2016.

453 Jin, P., Wang, T. F., Liu, N. N., Dupont, S., Beardall, J., Boyd, P. W., Riebesell, U., and

454 Gao, K. S.: Ocean acidification increases the accumulation of toxic phenolic  
455 compounds across trophic levels, *Nat. Commun.*, 6, 1-6, 2015.

456 Johnson, M. D., and Carpenter, R. C.: Nitrogen enrichment offsets direct negative effects  
457 of ocean acidification on a reef-building crustose coralline alga, *Biol. Letters*, 14,  
458 1-5, 2018.

459 Li, F. T., Wu, Y. P., Hutchins, D. A., Fu, F. X., and Gao, K. S.: Physiological responses of  
460 coastal and oceanic diatoms to diurnal fluctuations in seawater carbonate chemistry  
461 under two CO<sub>2</sub> concentrations, *Biogeosciences*, 13, 6247-6259, 2016.

462 Li, F. T., Beardall, J., and Gao, K. S.: Diatom performance in a future ocean: interactions  
463 between nitrogen limitation, temperature, and CO<sub>2</sub>-induced seawater acidification,  
464 *ICES J. Mar. Sci.*, 75, 1451-1464, 2018.

465 Li, G., Gao, K. S., Yuan, D. X., Zheng, Y., and Yang, G. Y.: Relationship of  
466 photosynthetic carbon fixation with environmental changes in the Jiulong River  
467 estuary of the South China Sea, with special reference to the effects of solar UV  
468 radiation, *Mar. Pollut. Bull.*, 62, 1852-1858, 2011.

469 Li, H. X., Xu, T. P., Ma, J., Li, F. T., and Xu, J. T.: Physiological responses of  
470 *Skeletonema costatum* to the interactions of seawater acidification and the  
471 combination of photoperiod and temperature, *Biogeosciences*, 18, 1439-1449, 2021.

472 Li, W., Gao, K., and Beardall, J.: Nitrate limitation and ocean acidification interact with  
473 UV-B to reduce photosynthetic performance in the diatom *Phaeodactylum*



474 *tricornutum*, Biogeosciences, 12, 2383-2393, 2015.

475 Lu, Z., Gan, J., Dai, M., Zhao, X. and Hui, C. R.: Nutrient transport and dynamics in the  
476 South China Sea: A modeling study. Prog. Oceanogr., 183, 102308, 2020.

477 McNicholl, C., Koch, M. S., and Hofmann, L. C.: Photosynthesis and light-dependent  
478 proton pumps increase boundary layer pH in tropical macroalgae: A proposed  
479 mechanism to sustain calcification under ocean acidification, J. Exp. Mar. Biol.  
480 Ecol., 521, 1-12, 2019.

481 Moreau, S., Penna, A. D., Llorc, J., Patel, R., Langlais, C., Boyd, P. W., Matear, R. J.,  
482 Phillips, H. E., Trull, T. W., Tilbrook, B. and Lenton, A.: Eddy-induced carbon  
483 transport across the Antarctic Circumpolar Current. Global Biogeochem. Cy., 31,  
484 1368-1386, 2017

485 Mostofa, K.M., Liu, C.Q., Zhai, W., Minella, M., Vione, D., Gao, K., Minakata, D.,  
486 Arakaki, T., Yoshioka, T., Hayakawa, K. and Konohira, E.: Reviews and Syntheses:  
487 Ocean acidification and its potential impacts on marine ecosystems, Biogeosciences,  
488 13, 1767-1786, 2016.

489 Pierrot, D., Wallace, D.W. R., and Lewis, E.: MS Excel program developed for CO<sub>2</sub>  
490 system calculations. ORNL/CDIAC-105a, Carbon Dioxide Information Analysis  
491 Center, Oak Ridge National Laboratory, US Department of Energy, Oak Ridge,  
492 Tennessee, USA., 2006.

493 Porra, R. J.: The chequered history of the development and use of simultaneous equations

494 for the accurate determination of chlorophylls a and b, *Photosynth. Res.*, 73,  
495 149-156, 2002.

496 Raven, J. A., and Beardall, J.: CO<sub>2</sub> concentrating mechanisms and environmental change,  
497 *Aquat. Bot.*, 118, 24-37, 2014.

498 Schippers, P., Lüring, M., and Scheffer, M.: Increase of atmospheric CO<sub>2</sub> promotes  
499 phytoplankton productivity, *Ecol. Lett.*, 7, 446-451, 2004.

500 Shi, D. L., Hong, H. Z., Su, X., Liao, L. R., Chang, S. W., and Lin, W. F.: The  
501 physiological response of marine diatoms to ocean acidification: Differential roles of  
502 seawater pCO<sub>2</sub> and pH, *J. Phycol.*, 55, 521-533, 2019.

503 Taylor, A. R., Brownlee, C., and Wheeler, G. L.: Proton channels in algae: Reasons to be  
504 excited, *Trends Plant Sci.*, 17, 675-684, 2012.

505 Tortell, P. D., Rau, G. H., and Morel, F. M. M.: Inorganic carbon acquisition in coastal  
506 Pacific phytoplankton communities, *Limnol. Oceanogr.*, 45, 1485-1500, 2000.

507 Tremblay, J. E., Michel, C., Hobson, K. A., Gosselin, M., and Price, N. M.: Bloom  
508 dynamics in early opening waters of the Arctic Ocean. *Limnol. Oceanogr.*, 51,  
509 900-912, 2006.

510 Riebesell, U., Aberle-Malzahn, N., Achterberg, E. P., Algueró-Muñiz, M.,  
511 Alvarez-Fernandez, S., Arístegui, J., Bach, L. T., Boersma, M., Boxhammer, T.,  
512 Guan, W. C., Haunost, M., Horn, H. G., Loscher, C. R., Ludwig, A., Spisla, C.,  
513 Sswat, M., Stange, P., and Taucher, J.: Toxic algal bloom induced by ocean

514 acidification disrupts the pelagic food web, *Nat. Clim. Change*, 8, 1082-1086, 2018.

515 Wu, Y., Gao, K., and Riebesell, U.: CO<sub>2</sub>-induced seawater acidification affects  
516 physiological performance of the marine diatom *Phaeodactylum tricornutum*,  
517 *Biogeosciences*, 7, 2915-2923, 2010.

518 Wu, Y., Campbell, D. A., Irwin, A. J., Suggett, D. J., and Finkel, Z. V.: Ocean  
519 acidification enhances the growth rate of larger diatoms. *Limnol. Oceanogr.*, 59,  
520 1027-1034, 2014.

521 Wu, Y. P., and Gao, K. S.: Combined effects of solar UV radiation and CO<sub>2</sub>-induced  
522 seawater acidification on photosynthetic carbon fixation of phytoplankton  
523 assemblages in the South China Sea. *Chinese Sci. Bull.*, 55, 3680-3686, 2010.

524 Xiao, W. P., Wang, L., Laws, E., Xie, Y. Y., Chen, J. X., Liu, X., Chen, B. Z., and Huang,  
525 B. Q.: Realized niches explain spatial gradients in seasonal abundance of  
526 phytoplankton groups in the South China Sea, *Prog. Oceanogr.*, 162, 223-239, 2018.

527 Xie, S., Lin, F., Zhao, X. and Gao, G.: Enhanced lipid productivity coupled with carbon  
528 and nitrogen removal of the diatom *Skeletonema costatum* cultured in the high CO<sub>2</sub>  
529 level. *Algal Res.* 61, 102589, 2022.

530 Xu, J. K., Sun, J. Z., Beardall, J., and Gao, K. S.: Lower salinity leads to improved  
531 physiological performance in the coccolithophorid *Emiliana huxleyi*, which partly  
532 ameliorates the effects of ocean acidification, *Front. Mar. Sci.*, 7, 1-18, 2020.

533 Xu, Z. G., Gao, G., Xu, J. T., and Wu, H. Y.: Physiological response of a golden tide alga

534 (*Sargassum muticum*) to the interaction of ocean acidification and phosphorus  
535 enrichment, *Biogeosciences*, 14, 671-681, 2017.

536 Yang, G. Y., and Gao, K. S.: Physiological responses of the marine diatom *Thalassiosira*  
537 *pseudonana* to increased  $p\text{CO}_2$  and seawater acidity, *Mar. Environ. Res.*, 79,  
538 142-151, 2012.

539 Yoshimura, T., Nishioka, J., Suzuki, K., Hattori, H., Kiyosawa, H. and Watanabe, Y. W.:  
540 Impacts of elevated  $\text{CO}_2$  on organic carbon dynamics in nutrient depleted Okhotsk  
541 Sea surface waters. *J. Exp. Mar. Biol. Ecol.*, 395, 191-198, 2010.

542 Yu, P., Wang, Z. A., Churchill, J., Zheng, M., Pan, J., Bai, Y. and Liang, C.: Effects of  
543 typhoons on surface seawater  $p\text{CO}_2$  and air-sea  $\text{CO}_2$  fluxes in the northern South  
544 China Sea. *J. Geophys. Res-Oceans*, 125, p.e2020JC016258, 2020.

545 Yuan, X., He, L., Yin, K., Pan, G. and Harrison, P. J.: Bacterial distribution and nutrient  
546 limitation in relation to different water masses in the coastal and northwestern South  
547 China Sea in late summer. *Cont. Shelf Res.*, 31, 1214-1223, 2011.

548 Zhong, Y. P., Liu, X., Xiao, W. P., Laws, E. A., Chen, J. X., Wang, L., Liu, S. G., Zhang,  
549 F., and Huang, B. Q.: Phytoplankton community patterns in the Taiwan Strait match  
550 the characteristics of their realized niches, *Prog. Oceanogr.*, 186, 1-15, 2020.

551 **Figure captions**

552 **Fig. 1** Sampling stations for the incubation experiments in the Taiwan Strait and the  
553 South China Sea during three cruises. Taiwan Strait cruise was conducted in July 2016  
554 (red dots), South China Sea Basin cruise were conducted in September 2016 (blue dots)  
555 and Western South China Sea cruise was conducted in September 2017 (black dots).

556 **Fig. 2** Temperature ( $^{\circ}\text{C}$ , panel a), salinity (panel b), pH (panel c), total alkalinity ( $\mu\text{mol}$   
557  $\text{L}^{-1}$ , panel d), and  $\text{CO}_2$  ( $\mu\text{mol kg}^{-1}$  SW, panel e) in surface seawater and mean PAR  
558 intensity ( $\text{W m}^{-2} \text{s}^{-1}$ , panel f) during the PP incubation experiments.

559 **Fig. 3** Chl *a* concentration ( $\mu\text{g L}^{-1}$ ) in the Taiwan Strait and the South China Sea during  
560 research cruises.

561 **Fig. 4** Surface primary productivity ( $\mu\text{g C } (\mu\text{g Chl } a)^{-1} \text{ d}^{-1}$ ) in the Taiwan Strait and the  
562 South China Sea during research cruises.

563 **Fig. 5** Ocean acidification (pH decreases of 0.4 units) induced changes (%) of surface  
564 primary productivity in the Taiwan Strait and the South China Sea. Red-yellow shading  
565 represents a positive effect on PP and blue-purple shading represents a negative effect.

**Fig. 6** Ocean acidification (pH decreases of 0.4 units) induced changes (%) on surface primary productivity in the South China Sea as a function of ambient pH (a), PAR (b), and salinity (c). The dotted lines represent 95% confidence intervals.

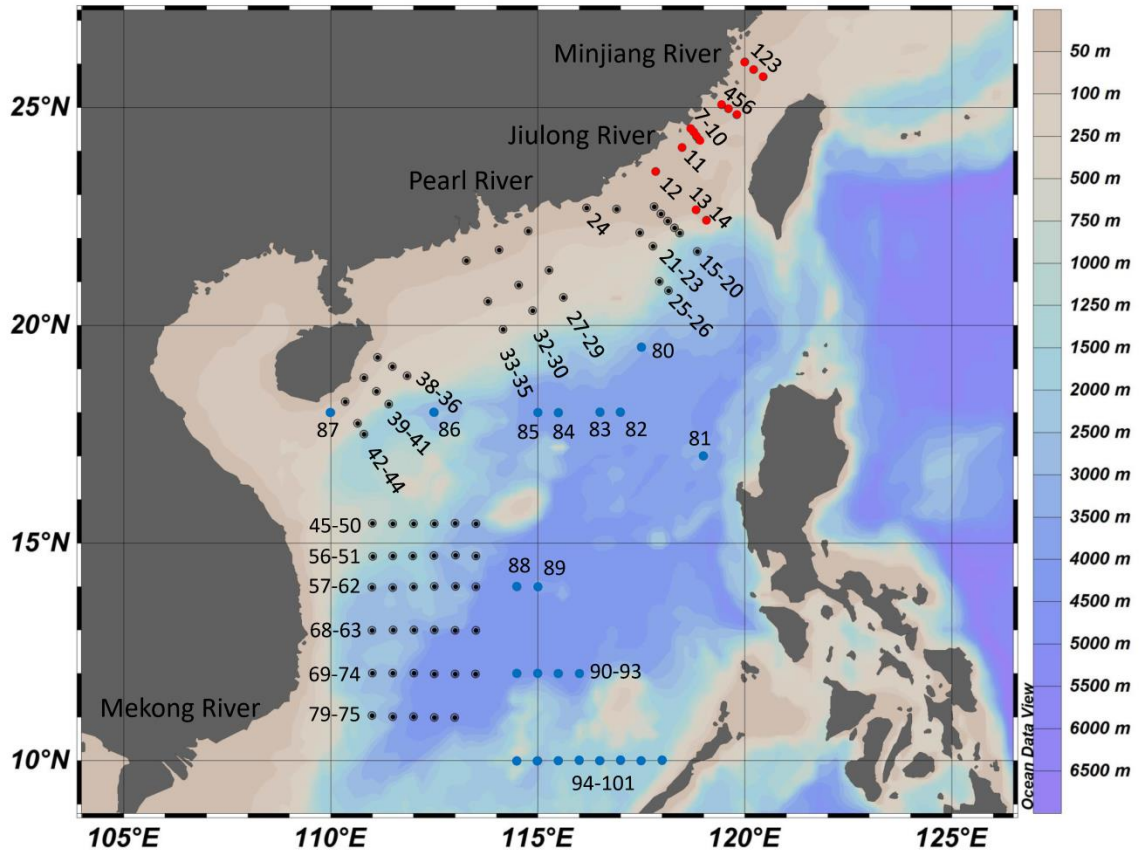


Fig. 1

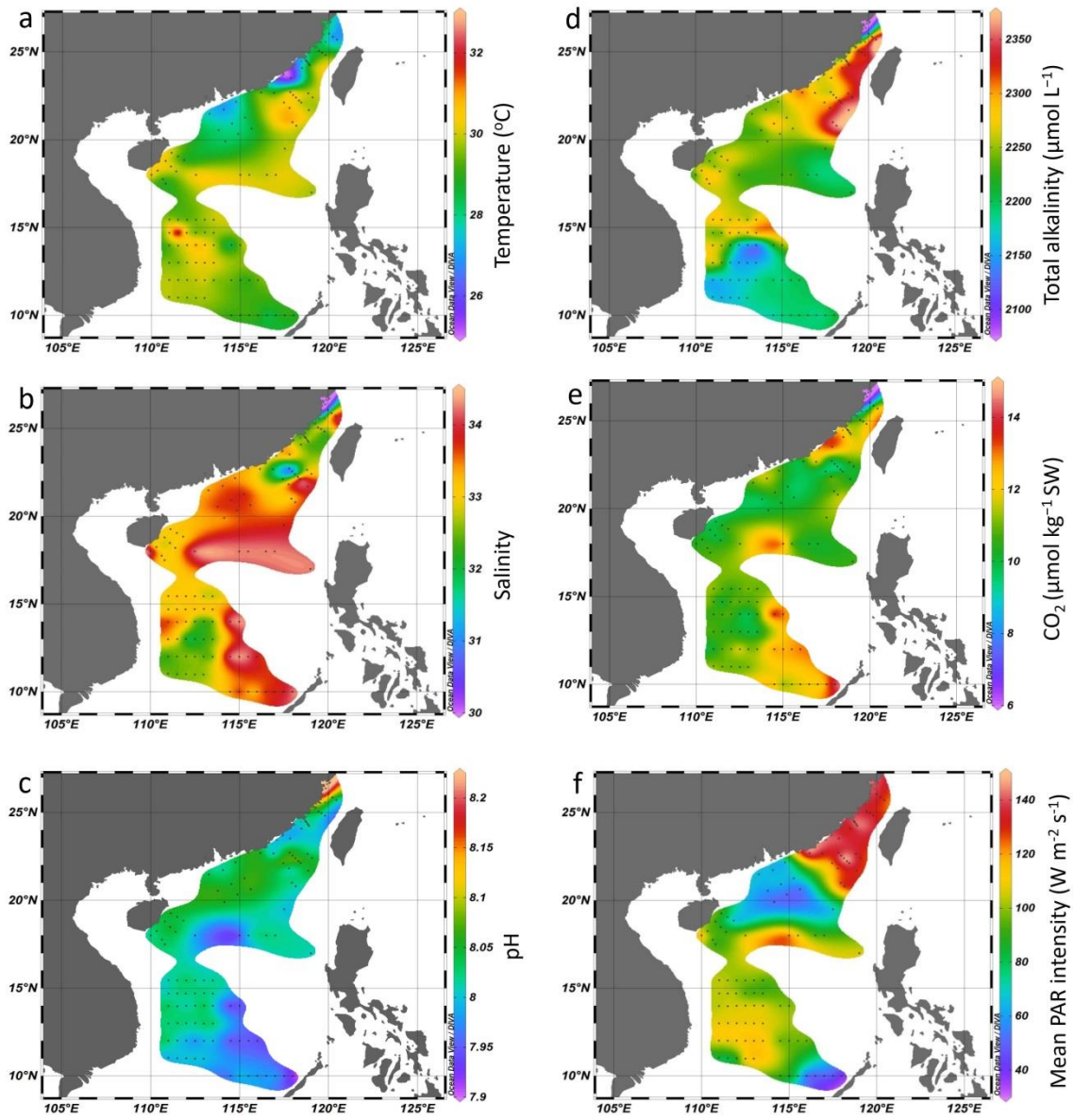


Fig. 2



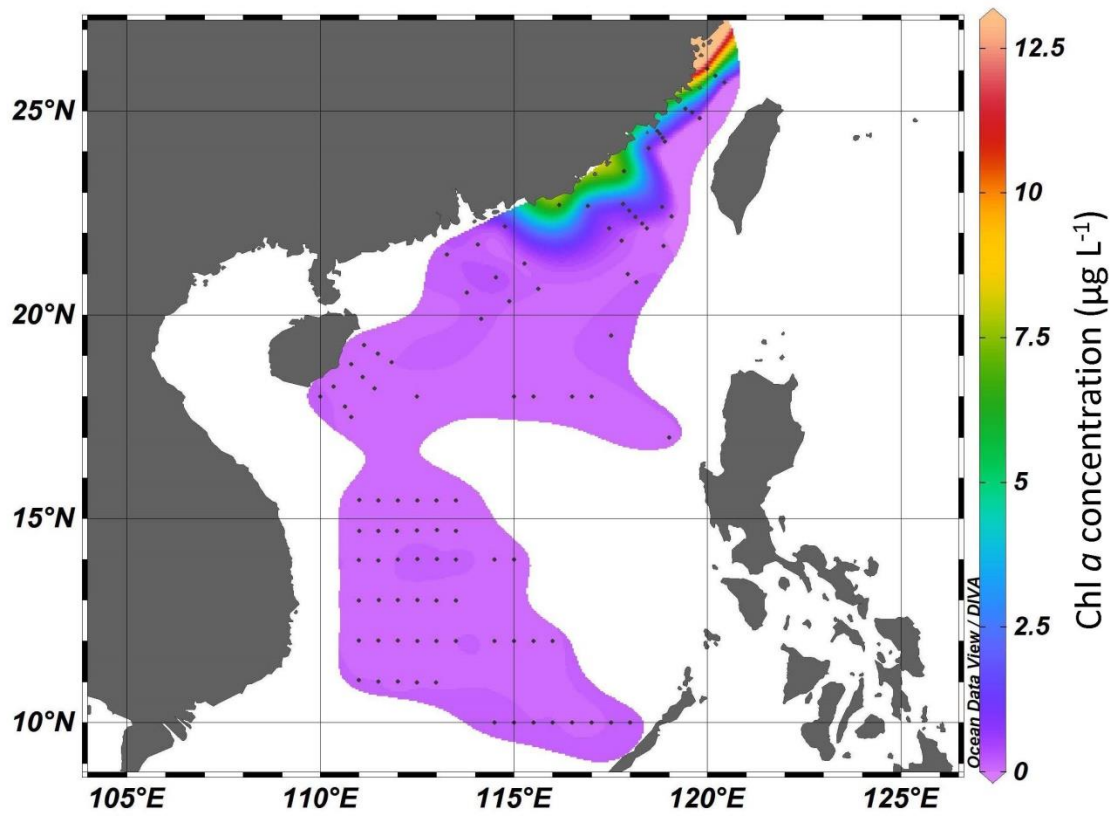


Fig. 3

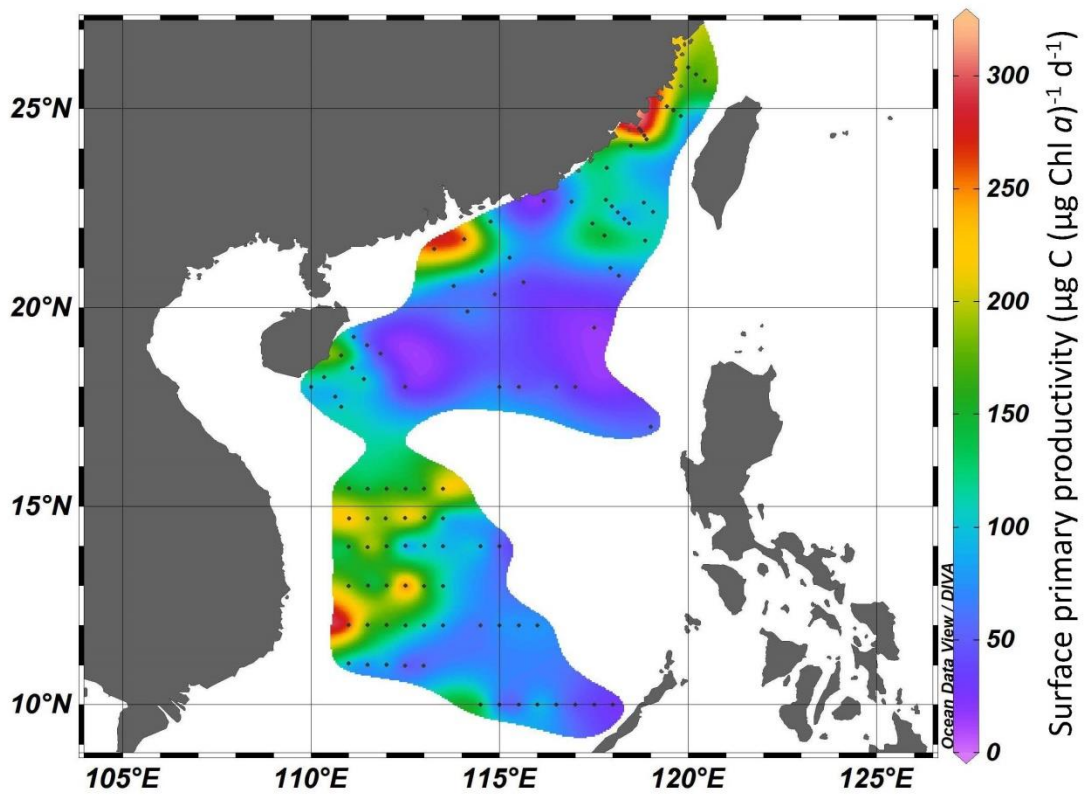


Fig. 4

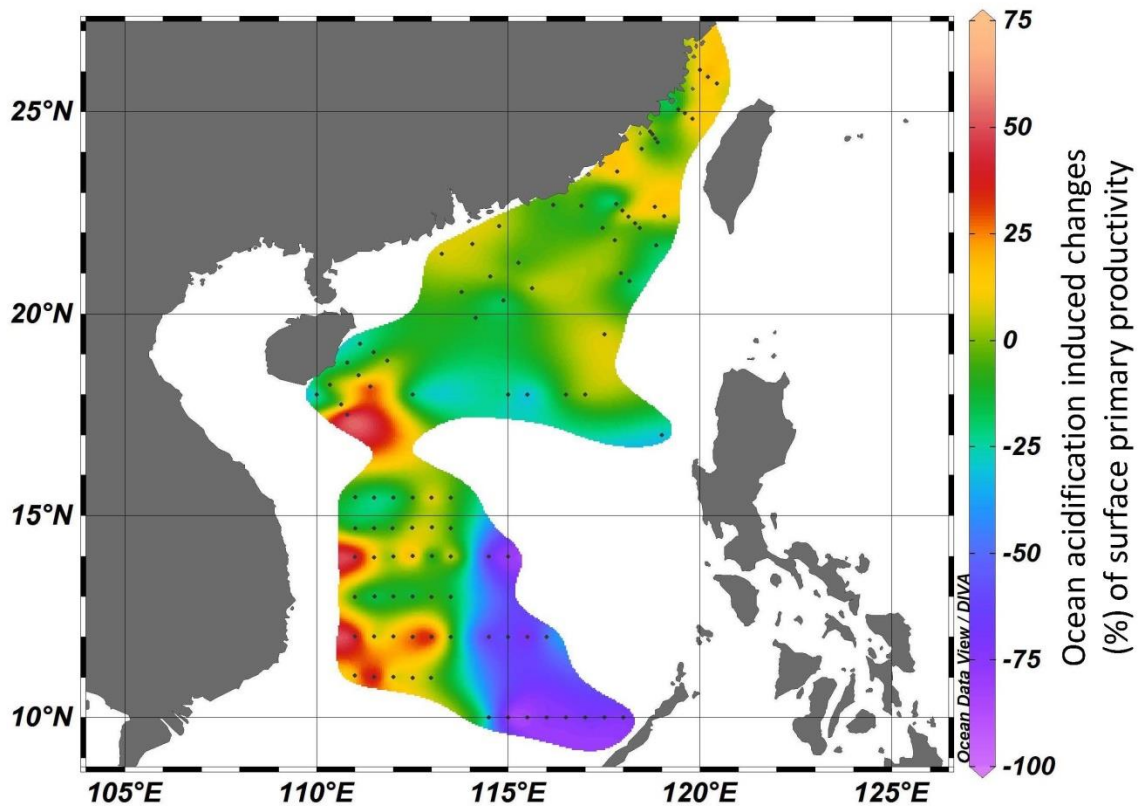


Fig. 5

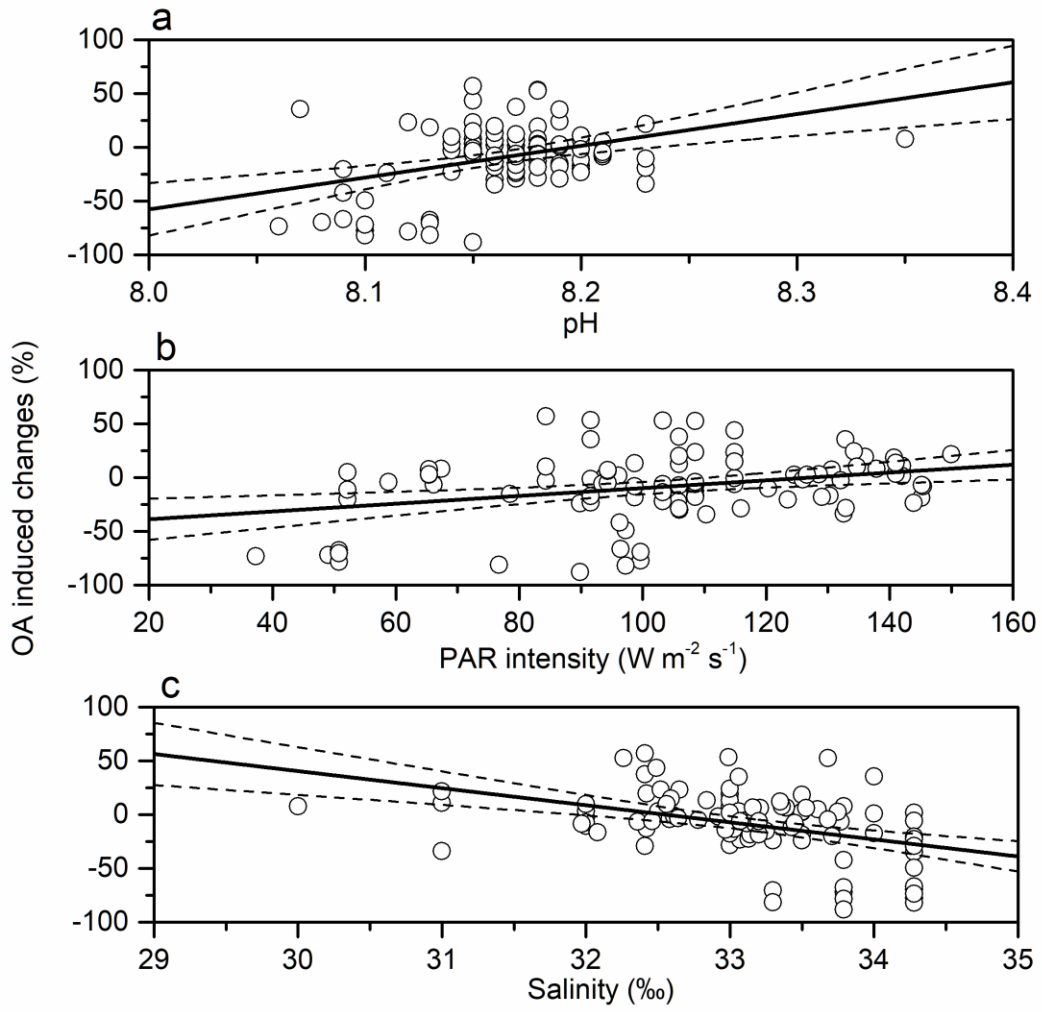


Fig. 6